

## The removal of diazinon from aqueous solution by chitosan/carbon nanotube adsorbent

T. Taghizade Firozjaee\*, N. Mehrdadi, M. Baghdadi, G.R. Nabi Bidhendi

*Department of Environmental Engineering, Graduate Faculty of Environment, University of Tehran, Tehran, Iran, Tel. +98 21 61113171, Fax +98 21 66407719, email: taghizade.eng@gmail.com, t.taghizade@ut.ac.ir (T.T. Firozjaee), mehrdadi2@yahoo.com (N. Mehrdadi), m.baghdadi@ut.ac.ir (M. Baghdadi), ghhendi@ut.ac.ir (G.R.N. Bidhendi)*

Received 14 October 2016; Accepted 6 April 2017

### ABSTRACT

The removal of diazinon using low-cost sorbent Chitosan/Carbon Nanotube (CHN-CNT) from aqueous solutions has been investigated in the present study. A protected cross linking method was used to synthesis of CHN-CNT with 2.5% of MWCNT. MWCNT is a promising candidate for improving chitosan mechanical properties. Scanning electron microscopy (SEM), infrared spectroscopy (FT-IR) and Thermogravimetric analyzer (TGA) were used to characterize the prepared adsorbent. Tests were done to evaluate the effects of solution pH, the amount of CHN-CNT, diazinon concentration, contact time and solution temperature on adsorption of diazinon onto CHN-CNT. Results showed that CHN-CNT at a low amount of 0.5 g/L, in contact time 60 min and pH 5.5, could remove 82.5% of the diazinon at initial concentration 5 mg/L. The Langmuir, Freundlich and Sips isotherm models were used to analyze the equilibrium experimental data. Equilibrium adsorption isotherm data exhibited better fit to the Sips isotherm model, where the heterogeneity factor ( $n = 0.66$ ) indicated heterogeneous adsorption characteristics, with a maximum adsorption capacity of 222.86 mg/g. Also the experimental adsorption data was fitted well to the pseudo-second-order model. Overall, the use of CHN-CNT due to the easier to prepare, high performance in adsorption, simple and effective regeneration make CHN-CNT as a promising adsorbent to eliminate the pesticide from contaminated streams.

*Keywords:* Diazinon; Chitosan; Carbon nanotube; Adsorption; Isotherm

### 1. Introduction

Organophosphate pesticides are a major class of pesticides to control a variety of insects in agriculture. Diazinon is a member of the organophosphate insecticides classified by the World Health Organization (WHO) as “moderately hazardous” Class II [1]. It is effective against adult and juvenile forms of flying insects, crawling insects, acarions and spiders [2]. This compound is nerve poisons, highly toxic to animals and humans. Specifically, neurotoxicity effects of diazinon are attributed to its inhibition of the enzyme acetylcholinesterase [3]. Residues of diazinon has been detected in the surface and ground water due to its high usage frequency in agriculture [4].

Several techniques have been used for the elimination of pesticides from aqueous solution including adsorption, advanced oxidation processes, coagulation, membrane filtration and biodegradation [5–13]. Adsorption has been found to be superior to other techniques for water and waste water treatment because of initial cost, flexibility, and simplicity of design, ease of operation, and elimination of toxic organic contaminants. Adsorption also does not result in the formation of harmful substances [14]. This process is a surface phenomenon that depends on the number of sites available, porosity and specific surface area of adsorbent as well as various types of interactions.

Various adsorbents have been used to remove different types of pesticides. Chitosan is a glucosamine bipolymer that is a good adsorbent to remove various kinds of organic pollutant. Chitosan is a naturally abundant muco-

\*Corresponding author.

polysaccharide that synthesized from the deacetylation of chitin. It can be extracted from crustacean shell such as fungi, insects and other crustaceans [15]. Because of its unique properties, such as non-toxicity, biodegradability, and biocompatibility, chitosan has a wide range of applications in various fields. Chitosan can be used as an excellent natural adsorbent with powerful adsorptive capacity due to presence hydroxyl (–OH) and amino (–NH<sub>2</sub>) functional groups of chitosan [16]. Amino groups of chitosan can be cationized in the acidic media and adsorb anionic organic compound strongly by electrostatic attraction [17]. Despite excellent performance of chitosan as an adsorbent, poor mechanical properties of CS hydrogel beads limits their commercial application as an adsorbent [18,19]. Various chemical methods, including poly amination, chemical cross-linking and carboxy alkyl substitution, have been performed to increase the mechanical strength of CS hydrogel beads. But these processes may not satisfactorily improve mechanical stability [20].

An effective method for improving the physico/chemical properties of chitosan is incorporation with inorganic fillers including silica and clay nanoparticles, Hydroxyapatite and calcium phosphate cements that are often used to reinforce the chitosan matrix [19,21,22]. Carbon nanotubes (CNTs) have been consider as favorable reinforcing fillers for chitosan to achieve high performance and multi functions, because of its excellent mechanical, electrical and thermal properties. The incorporation of CNTs in chitosan has been shown to improve the improvement of mechanical and thermal properties compared with those of neat chitosan, which may broaden the applications of chitosan [18–20,23,24].

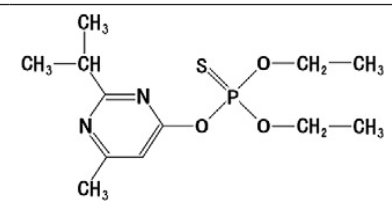
The aim of the present study is to explore the performance of CS/CNT to remove diazinon from aqueous solution. Some characterization studies, such as scanning electron microscopy (SEM), infrared spectroscopy (FT-IR) and Thermogravimetric analyzer (TGA) were used. The effect of various factors such as temperature, contact time and concentration and pH were investigated. The adsorption data were fitted to the Freundlich, Langmuir and Sips isotherm equations. The adsorption kinetics of diazinon in water on adsorbent was also analyzed by using pseudo first order and pseudo-second-order kinetic models.

## 2. Materials and methods

### 2.1. Materials

Diazinon for the experiment was supplied by Sigma-Aldrich. The properties of diazinon are presented in Table 1 [11]. A stock solution (1,000 mg/L diazinon) was prepared by dissolving appropriate amount of the diazinon in deionized water and kept in a refrigerator at 4°C until use. Pristine multi-wall CNTs were purchased from Nanosav Company (Tehran Province, Iran). According to the data obtained from the company, the length of multi-wall carbon nanotube (MWCNT) was <10 μm, the amount of amorphous carbon was <5%, and the outer diameter ranged from 10 to 30 nm which was synthesized by the special chemical vapor deposition (CVD) method using iron, cobalt, and molybdenum as the catalyst. Medium molecular weight chitosan (MMWC) powder was pur-

Table 1  
Characteristics of diazinon insecticide used in this study [11]

Parameter	Character/value
Molecular structure	
CAS number	333-41-5
Chemical formula	C <sub>12</sub> H <sub>21</sub> N <sub>2</sub> O <sub>3</sub> PS
Molecular weight	304.35 g/mol
Solubility in water	40 mg/L at 25°C
Octanol-water partition coefficient (log K <sub>ow</sub> )	3.40
Dissociation constant (pKa)	2.6 at 25 °C

chased Sigma-Aldrich. All of the other reagents nitric acid (Synth, 65%), acetic acid (Synth, 99%), Glutaraldehyde (Synth, 25%), methanol (Synth, 99.9%) were purchased from Merck.

### 2.2. Adsorption experiments

Adsorption studies were performed in the closed batch system prepared in 100 mL flasks, closed with a cap. For each adsorption experiment, 25 mL of the diazinon solution was transferred to the flask, the solution pH level was adjusted to the desired value; the given amount of CHN-CNT was added to the solution, and the suspension was put on the magnetic device and stirred at 150 rpm for the preferred time. Cellulose acetate filter with 0.20 μm pore size was used to prepare solutions before injection to HPLC. The selected variables and their limits were as follows; solution pH (3–8), the amount of CHN-CNT (0.4–0.6 g/L), diazinon concentration (5–50 mg/L), contact time (10–300 min), solution temperature (15–45°C). The suspensions were carried to the desired pH by the addition of 0.1 M NaOH and 0.1 M HCl. All the experiments were performed in duplicate to ensure data reproducibility

### 2.3. Analysis

Scanning electron microscopy (DSM-960A, Zeiss) was used to study the morphology of CHN and CHN-CNT. Fourier Transform Infrared Spectrophotometer (Tensor 27, Equinox 55, Bruker) was used to detect any functional groups of CHN and CHN-CNT. Thermogravimetric analysis was performed using TG analyser (STA504 from BHR Co., Germany). The runs were carried out in the temperature range of 22–600°C with a heating rate of 10°C min<sup>-1</sup> in air. The concentration of diazinon was determined using a HPLC (Agilent 1100 Series) with C18 column (250 × 4.6 × 5) and a UV detector at a wavelength of 248 nm. The mobile

phase was a mixture of acetonitrile and water with a volumetric ratio of 65/35 with an injection flow rate of 1 mL/min. The pH was measured using a pH meter (Sense Ion 378, Hack). Temperatures of solutions were determined with a thermometer. Ultrasound bath (HWASHIN, Power Sonic 420, 50HZ, 700 W, Seoul, Korea) was used for solution dispersion. Calculations of amounts of adsorption of diazinon onto CHN-CNT were based on removal efficiency (R) and adsorption capacity ( $q_e$ ) as follows:

$$R = \frac{(C_0 - C_e)}{C_0} \times 100 \quad (1)$$

$$q_e = \frac{V(C_0 - C_e)}{M} \quad (2)$$

where  $q_e$  is the amount of diazinon adsorbed by CHN-CNT (mg/g),  $C_0$  and  $C_e$  are the initial and equilibrium liquid-phase concentrations of diazinon (mg/L), respectively,  $V$  is the solution volume (L), and  $M$  is the weight of CHN-CNT used in the adsorption tests (gr).

#### 2.4. Preparation of the CHN-CNT adsorbent

##### 2.4.1. CNT oxidized

For polymer composites applications, CNT functionalization is needed to improve dispersion as well as to improve the interfacial strength and composite mechanical performance [19,25]. Since chitosan contains amino groups, hydrogen-bonding between the functionalized MWCNTs and chitosan is formed. Various impurities such as amorphous carbon, graphitic plates, and metal catalysts can reduce the adsorption effects of MWCNT thus chemical oxidation is recognized as an efficient method for CNT purification, promoting dispersion and surface activation and the solubility in polar media at the same time [25–27].

Acidic oxidation methods have been widely reported as an effective method to purify and functionalize the surface of carbon nanotubes (CNTs) [25]. Nitric acid is effective and strong acid for oxidation of CNTs that introduced functional groups such as carboxyl, carbonyl, and hydroxyl on CNTs [25,26,28]. Since temperature and contact time are important factors in oxidation and solubility of CNTs, different conditions were studied. The optimum condition for oxidation was observed at 140°C for 5 h due to best dispersibility of CNTs in deionized water [29]. For oxidation of CNTs, 4 g of pristine MWCNT was dispersed in 150 ml of HNO<sub>3</sub> (Synth, 65%) for periods of time (5 h) and at temperatures (140°C). Then, it was centrifuged for 10 min at 5,000 rpm. The solid residue was washed with deionized water to remove the excess nitric acid. Finally, it was dried under vacuum for 72 h.

##### 2.4.2. Synthesis of the CHN-CNT adsorbent

To make MWCNT suspension, 60 mg of MWCNT was first suspended in 40 mL deionized water. MWCNT suspension was homogenized in ultrasonic bath for 90 min at 35°C. CS solution was separately made by dissolving 2.5 g of CS into 100 mL deionized water and 1.5 ml 1% acetic acid. Using a magnetic stirrer, CS solution was completely

mixed for 24 h. In two stages MWCNT suspension was added to CS solution and homogenized in ultrasonic bath for 60 min at 35°C to achieve a final CS concentration of 2.5%. The final weight ratio of CNTs to CS in all of the experiments was 2.5%. Then the prepared dispersed solution was injected through a 0.2-mm-diameter syringe at a 1 rpm flow rate into a coagulation solution bath (H<sub>2</sub>O/MeOH/NaOH 4 : 5 : 1 w/w/w) at room temperature for 24 h with continuous stirring. The coagulated granules were then washed several times with deionized water. Then a protected-cross linking method with glutaraldehyde was used. Cross-linking agents do not only stabilize chitosan in acid solutions so it improves its mechanical properties [30]. The aminogroups of chitosan causes that chitosan can easily dissolve in various dilute acid solutions to yield a hydrogel in water. Thus, it is necessary in solubilization method such as cross linking treatment for applying chitosan to an adsorbent gel [31]. The cross linking was performed though C=N bond formation between the amine groups of CHN and the aldehyde terminals of the glutaraldehyde. The related reaction was carried out by the immersion of granular adsorbent in 25% glutaraldehyde (at the mass ratio of 2:1) at room temperature for 24 h. Then granular adsorbent was washed several times with deionized water. Finally, it was dried under vacuum for 72 h [32–34].

### 3. Results and discussion

#### 3.1. Characterization of adsorbent

##### 3.1.1. Morphological study

The SEM images shown in Fig. 1(A) and (B) correspond to CHN, oxidized MWCNT and Fig. 1(C) and (D) correspond to CHN-CNT, respectively. According to Fig. 1(D), surface of CHN-CNT illustrates a non-uniform coating of MWCNTs on chitosan including of CNT fibers that is different from the surface of the pristine chitosan. An electrostatic interaction between the positively charged polycation of CS and the negatively charged CNTs is induced and it would decrease the van der Waals forces among CNT bundles by wrapping the CNTs in polymerchains [33].

##### 3.1.2. Fourier transform infrared (FTIR) analysis

The infrared spectra of CHN and CHN-CNT are shown in Fig. 2. The FTIR spectra of pure chitosan (a spectrum) exhibit bands at 3545 cm<sup>-1</sup> and 3379 cm<sup>-1</sup> due to the stretching vibration mode of O–H and N–H groups. The peaks at 2936 cm<sup>-1</sup> is typical of C–H stretch vibration, while the band at 1652 cm<sup>-1</sup> is due to the amide group (C=O stretching of N-acetyl groups), 1378 cm<sup>-1</sup> peak is due to the COO– group in carboxylic acid salt, 1035 cm<sup>-1</sup> stretching vibration of C–O–C in glucose circle [30]. The cross linking reaction for CHN-CNT was confirmed by observation of a peak at 1587 cm<sup>-1</sup> which corresponds to imine C=N bond [34,35]. The stretching at 1720 cm<sup>-1</sup> is due to free-aldehydic bonds [36]. Also due to the presence of oxidized CNTs in CHN-CNT, the stretching vibration of functional groups C–H, COO– and C–O at 2936 cm<sup>-1</sup>, 1378 cm<sup>-1</sup> and 1035 cm<sup>-1</sup> peak, respectively, increased.

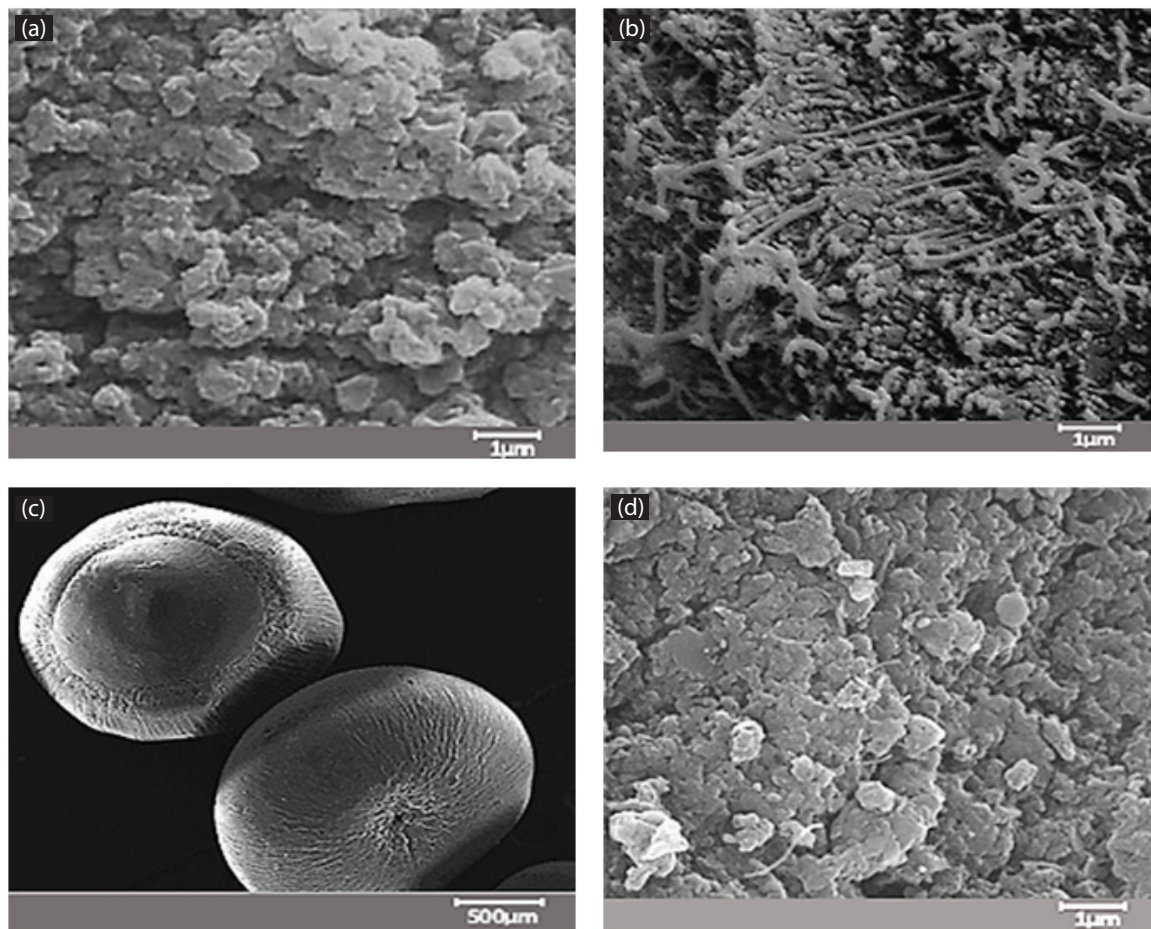


Fig. 1. SEM image of (A) Pristine chitosan, (B) oxidized MWCNT, (C) and (D) Chitosan-MWCNT 2.5% (CHN-CNT).

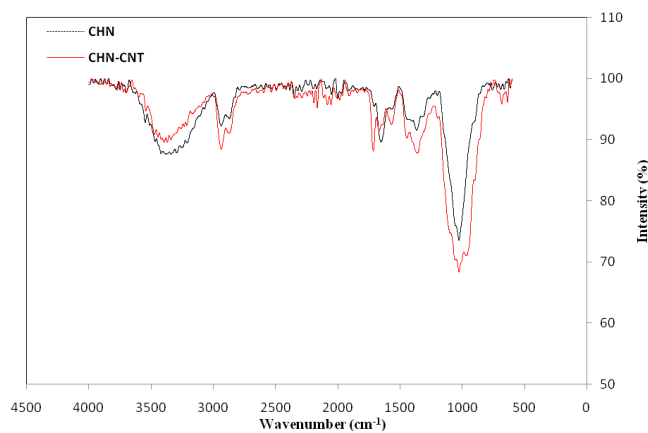


Fig. 2. FTIR spectra of CHN and CHN-CNT.

### 3.1.3. Thermogravimetric analyzer (TGA)

The thermal behavior of CHN and CHN-CNT by thermogravimetric analysis (TGA) are presented in Fig. 3. According to Fig. 3, for CHN and CHN-CNT, there are two main weight loss stages in the range of 220–350°C and 400–500°C which are attributed to decomposition of saccharide rings of chitosan chain [37] and imine bond between glutar-

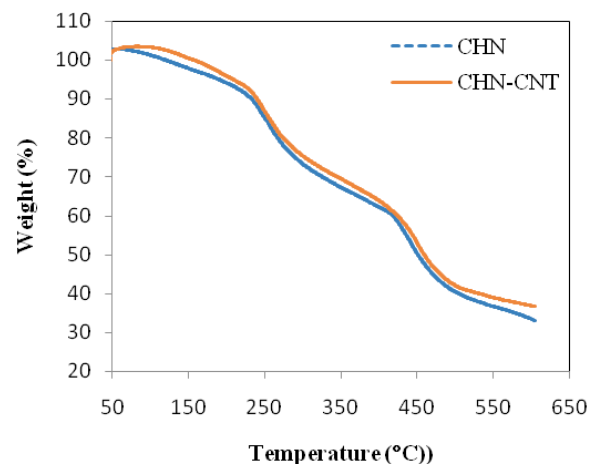


Fig. 3. Thermogravimetric analysis of CHN and CHN-CNT.

aldehyde and the glucosamine nitrogen of chitosan [38,39], respectively. The presence of carbon nanotubes in the chitosan enhanced the thermal stability in chitosan so that the percentage of decomposition decreased from 66.62% to 63.22% for the CHN and CHN-CNT, respectively. Thermal stability of chitosan-carbon nanotube composites was

investigated by some researchers [23,40,41]. In all instances, the results showed that the thermal stability of composites improved by addition of carbon nanotube.

### 3.1.4. Determination of pHpzc

The point zero charge (pHpzc), is the pH at which a particle carries no net electrical charge in the statistical mean. At pH values higher than the pHpzc, the surface of the CHN-CNT has negative charges and pH values below the pHpzc, there is a net positive charges on the CHN-CNT surface. In this study, the pHpzc were determined through measurement of pH changes of 0.1 M NaCl aqueous solutions containing CHN-CNT (0.5 mg/l) with initial pH in the range of 3–9 (adjusted by NaOH or HCl). The pHpzc of the CHN-CNT was about 5.9. The pHpzc of CHN-CNT indicated that its surface has positive charges at pH < 5.9 that can be due to presence of amine groups on surface of CHN-CNT.

### 3.2. Influence of solution pH

The effect of pH on the adsorption of diazinon by CHN-CNT is illustrated in Fig. 4. The pH was monitored in the range of 3 to 8 at 0.5 g/L CHN-CNT, 5 mg/L diazinon concentration and contact time of 60 min. As shown in Fig. 4, the adsorption of diazinon on CHN-CNT decreases with an increase in the pH. This behavior can be explained as follows; the surface of CHN-CNT is positively charged at a solution pH value below 5.9 (pHpzc). Also at low pH, diazinon molecules dissociate and convert into to anionic species (pKa = 2.6) [11,42]. The adsorption process is performed due to electrostatic attractions between the anionic species of diazinon and positively charged CHN-CNT particles at low pH. Also, due to presence of oxidized CNT fibers on the surface of CHN-CNT, several kinds of interactions contribute to diazinon attachment to oxidized CNT. At a low pH, oxidized CNT has hydrophobic surface due to the hydrogen bonding of COOH groups, leading to aggregated CNT [43,44]. Diazinon is a hydrophobic insecticide (Kow = 3.81), therefore it is thought that Hydrophobic attraction occur between diazinon and CNT with decreasing pH. Also,  $\pi$ - $\pi$  interactions might also have contributed to the aromatic fragments ( $\pi$  acceptors) of diazinon and the graphene sheets

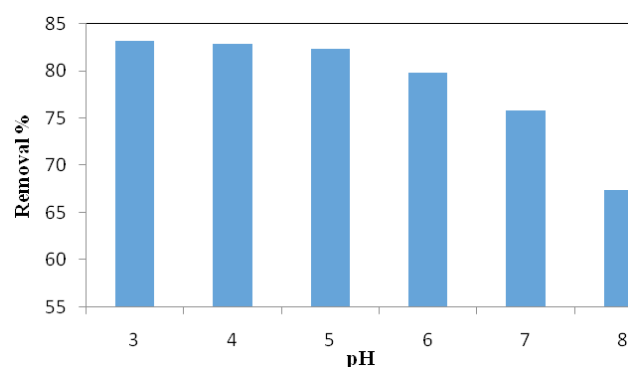


Fig. 4. Effect of solution pH on adsorption of diazinon onto CHN-CNT.

( $\pi$  donors) of carbon nanotubes [45,46]. The maximum diazinon adsorption on CHN-CNT (8.32 mg/g) occurred at pH 3. The result showed that pH plays an important role in the adsorption of diazinon by CHN-CNT.

### 3.3. Effect of amount of CHN-CNT and contact time

The influence of amount of CHN-CNT and contact time on diazinon removal constant concentration of diazinon 5 mg/L is presented in Fig. 5. According to Fig. 5, the adsorption of diazinon onto CHN-CNT has a fast stage at first which is followed by a slow stage until reaching equilibrium. In initial fast stage the available adsorption sites of CHN-CNT is high as time passes due to these sites are occupied the adsorption rate decreased. It can be seen the equilibrium time occur in 60 min for CHN-CNT. Also the removal of diazinon increased with an increased contact time for all three doses of CHN-CNT. In a short contact time of 10 min, 49.4%, 56.9%, and 70.2% of diazinon was removed with 0.4, 0.5, and 0.6 g CHN-CNT, respectively. The removal efficiency of diazinon increased to 62.3%, 80.8%, and 85.8% for 0.4, 0.5, and 0.6 g CHN-CNT, respectively, when the contact time was increased to 60 min. It can be explained, the greater CHN-CNT mass in a solution, the greater the number of adsorption sites available, consequently more diazinon molecules is able to interact with the available adsorption sites so improve diazinon removal [11]. The result showed that the CHN-CNT have a good potential in diazinon removal.

### 3.4. Adsorption isotherms

Adsorption isotherms are used to determine to quantify the interaction between solute and the adsorbents, critical in optimizing the purification process. Three equilibrium adsorption isotherms, namely Freundlich, Langmuir and Sips, have been studied. The Freundlich isotherm, which is an empirical equation for multi-layer adsorption of adsor-

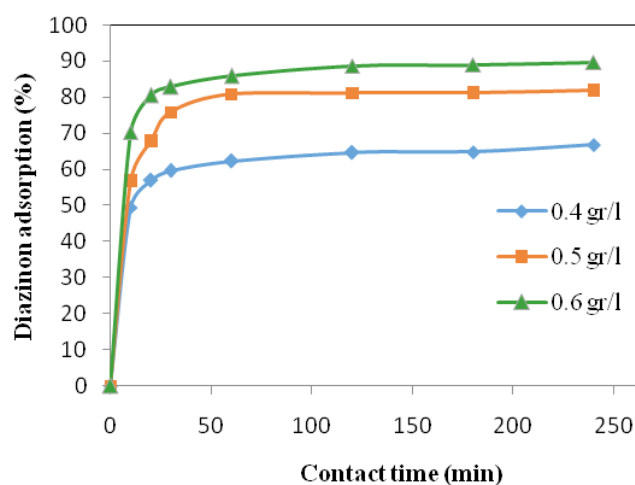


Fig. 5. Effect of amount of CHN-CNT on adsorption of diazinon onto CHN-CNT as a function of contact time (diazinon concentration: 5 mg/L; solution pH: 5.5; the amount of CHN-CNT : 0.4–0.6 g/L; contact time: 10–240 min; solution temperature: 25°C).

bate onto heterogeneous surfaces with a non-uniform distribution, can be expressed as follows: [47].

$$q_e = K_f C_e^{(1/n)} \quad (3)$$

Eq. (3) can be rearranged to obtain a linear form:

$$\log q_e = \log K_f + \left(\frac{1}{n}\right) \log C_e \quad (4)$$

where  $q_e$  (mg/g) is the amount of diazinon adsorbed onto CHN-CNT,  $C_e$  (mg/L) is the equilibrium concentration of diazinon in the liquid phase,  $n$  and  $K_f$  ((mg/g) (L/mg)<sup>(1/n)</sup>) are Freundlich constants that represent the adsorption intensity and adsorption capacity, respectively.

The Langmuir isotherm model describes mono-layer adsorption on homogeneous surface with no interaction between adjacent adsorbed solutes. The Langmuir isotherm is written as follows:

$$q_e = \frac{bQC_e}{1 + bC_e} \quad (5)$$

The linear form of Eq. (5) is:

$$\frac{c_e}{q_e} = \frac{c_e}{q_m} + \frac{1}{bq_m} \quad (6)$$

where  $b$  (L/mg) and  $Q$  (mg/g) is the Langmuir constant indicating mono-layer capacity and energy of adsorption, respectively. The Based on Langmuir isotherm, the separation factor  $R_L$  was estimated in the diazinon concentration range 5–50 mg/L using the relationship:

$$R_L = \frac{1}{(1 + bc_0)} \quad (7)$$

The computed values of  $R_L$  are in the ranges of 0.17–0.68 for diazinon, respectively. This indicates that sorption is favorable in nature [48].

Meanwhile the Sips isotherm model can be considered as a combination of Langmuir and Freundlich equations and expressed as follows [49]:

$$q_e = \frac{q_m (bC_e)^{1/n}}{1 + (bC_e)^{1/n}} \quad (8)$$

Eq. (8) can be linearized as:

$$\log\left(\frac{1}{q_e} - \frac{1}{q_m}\right) = \log\left(\frac{b^n}{q_m}\right) + \frac{1}{n} \log\left(\frac{1}{C_e}\right) \quad (9)$$

where  $q_m$  (mg/g) is maximum adsorption capacity,  $b$  (L/mg) is the affinity constant for adsorption and  $1/n$  is the

heterogeneity factor. If the value for  $1/n$  is less than one, it indicates that it is heterogeneous adsorbents, while values closer to or even one indicates that the adsorbent has relatively more homogeneous binding sites.

The equilibrium data fit well with non-linear and linear form of models. The obtained data from fitting the experimental equilibrium adsorption are presented in Table 2. According to Table 2, the non-linear form of models could estimate the experimental data slightly better than the linear forms. Equilibrium adsorption data could be better fitted with the Sips isotherm (Fig. 6). According to Table 2, the obtained data for the maximum adsorption capacity ( $q_m$ ) and heterogeneity factor ( $1/n$ ) are 222.86 mg/g and 0.66, respectively. The calculated values for  $1/n$  (0.66) showed that CHN-CNT beads are heterogeneous adsorbents. According to SEM images, surface of CHN-CNT illustrated a non-uniform distribution of MWCNTs in composite that causes a heterogeneity surface of CHN-CNT. Also some researcher showed that the cross-linked chitosan beads using glutaraldehyde have more heterogeneity on the surface compared to the chitosan beads [32,50].

### 3.5. Adsorption kinetics

In order to investigate the adsorption processes of diazinon on CHN-CNT, two well-known models, pseudo-first-order and pseudo-second-order kinetic model were employed to describe the adsorption process. The pseudo-first-order kinetic model is given as [12]:

$$\log \frac{q_e}{q_e - q_t} = \log \frac{K_1 t}{2.303} \quad (10)$$

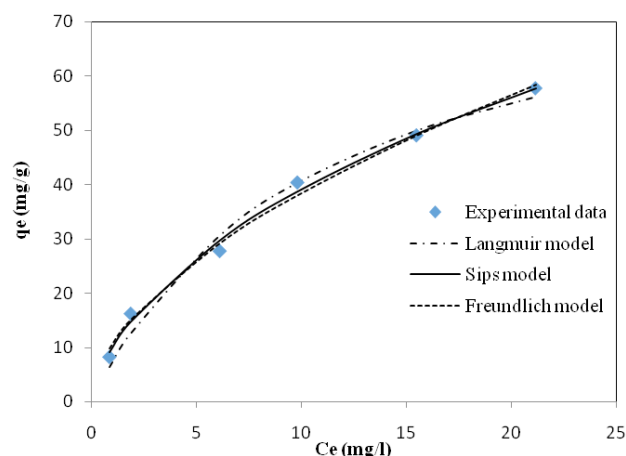


Fig. 6. Non-linear Freundlich (a), Langmuir (b) and Sips (c) model for the adsorption of diazinon onto CHN-CNT.

Table 2  
Information of diazinon adsorption isotherm onto CHN-CNT

Parameter	Freundlich isotherm			Langmuir isotherm				Sips isotherm			
	$n$	$R^2$		$b$	$R_L$	$R^2$	$b$	$1/n$	$R^2$		
Linear	9.77	1.69	0.988	77.51	0.118	0.14–0.62	0.965	222.86	0.01	0.67	0.992
Non-linear	10.62	1.79	0.998	85.22	0.091	0.17–0.68	0.996	222.86	0.0096	0.66	0.999

Eq. (10) can be rearranged to obtain a linear form:

$$\log(q_e - q_t) = \log q_e - \frac{K_1 t}{2.303} \quad (11)$$

The values of  $q_e$  and  $K_1$  are determined from the slope and intercept of the straight line. The pseudo-second-order kinetic model is presented as:

$$\frac{1}{q_t - q_e} = \frac{1}{q_e} + K_2 t \quad (12)$$

Eq. (12) can be linearized as:

$$\frac{t}{q_t} = \frac{1}{K_2 q_e^2} + \frac{1}{q_e} t \quad (13)$$

The value of  $q_e$  and  $K_2$  are determined from the slope and intercept of the straight line. Where,  $q_e$  and  $q_t$  refer to the amount of diazinon adsorbed (mg/g) at equilibrium and at any time,  $t$  (min), respectively.  $K_1$  and  $K_2$  are the equilibrium rate constants of the pseudo-first-order adsorption (1/min) and the pseudo-second-order adsorption (g/mg min), respectively. Fig. 7 shows the pseudo-first-order and pseudo-second-order kinetic model fitting to the experimental data for CHN-CNT at initial diazinon concentration 5 mg/L. The experimental amount of adsorption equilibrium ( $q_{e,exp}$ ), the rate constants of pseudo-first-order and pseudo-second-order kinetic ( $K_1$  and  $K_2$ ), the calculated amount of adsorption equilibrium ( $q_{e,cal}$ ) and the correlation coefficients ( $R^2$ ) are shown in Table 3.

A lower normalized standard deviation was obtained as follow[11]:

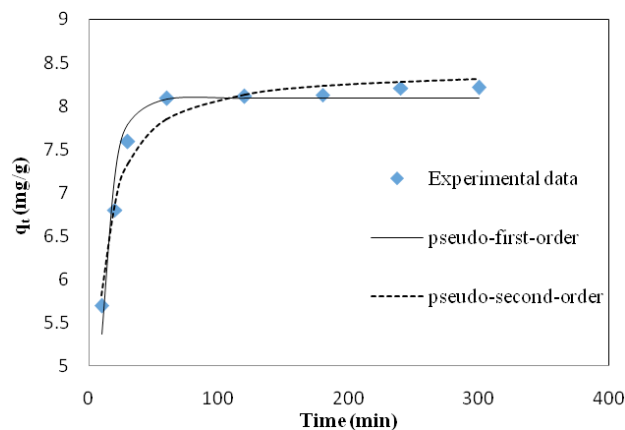


Fig. 7. Kinetic models for diazinon adsorption onto CHN-CNT at initial concentration 5 mg/L.

Table 3

Adsorption kinetic model rate constants for diazinon adsorption onto CHN-CNT

	Methods		Pseudo-first-order				Pseudo-second-order			
	$C_0$	Experimental	$K_1$	$R^2$			$K_2$	$R^2$		
Linear	5	8.2	0.025	0.739	6.91	0.155	0.034	0.999	8.33	0.0379
Non-linear	5	8.2	0.25	0.9993	8.088	0.0323	0.026	0.9996	8.43	0.0207

$$\Delta q = \sqrt{\frac{\sum [(q_{exp} - q_{model}) / q_{exp}]^2}{n - 1}} \quad (14)$$

The best model is based a higher determination coefficient ( $R^2$ ) and lower normalized standard deviation ( $\Delta q$ ). As observed in Table 3, the calculated amount of adsorption equilibrium ( $q_{e,cal}$ ) from pseudo-first-order and pseudo-second-order kinetic model for linear and non-linear methods are relatively close to the experimental amount of adsorption equilibrium ( $q_{e,exp}$ ). The pseudo-second-order kinetic model, as shown clearly in Fig .7, appeared to be the better fitting model because it has higher  $R^2$  and lower  $\Delta q$  than of the pseudo-first-order kinetic model. Several researches investigated the removal of pollutants by chitosan and carbon nanotube sorbents either individual or composite [20,24,29,32,51–54]. In many cases, the experimental data for adsorption could be well fitted by second-order kinetic model. The better fit of the pseudo-second-order model with the experimental data of diazinon adsorption onto CHN-CNT indicates that both adsorbate and adsorbent affected the adsorption [55,56]. Also as observed in Table 4, the non-linear forms of pseudo-first-order and models were more suitable than the linear forms for fitting the experimental data and estimating the kinetic parameters. Similar findings were reported in previous research [57].

### 3.6. Adsorption thermodynamic

The effect of temperature on the sorption of diazinon onto CHN-CNT was studied in the range of 288–318 K at initial concentration 5 mg/L and optimum conditions. The plot of  $\ln K_c$  verses  $1/K$  gives a straight line with a coefficient of determination ( $R^2$ ), 0.97 for diazinon as shown in Fig. 7. Thermodynamic parameters such as Gibbs free energy change  $\Delta G^\circ$  (KJ/mol), standard enthalpy change  $\Delta H^\circ$  (KJ/mol), and standard entropy change  $\Delta S^\circ$  (J/mol K) were estimated by the following equations [48]:

$$\Delta G^\circ = -RT \ln K_c \quad (15)$$

$$\frac{\Delta H^\circ}{RT} - \frac{\Delta S^\circ}{R} = \ln K_c \quad (16)$$

where  $K_c$  is the thermodynamic equilibrium constant of adsorption (L/gr),  $R$  is the gas constant (8.314 J/(k.mol)), and  $T$  is the absolute temperature (K). The values of  $\Delta H^\circ$  and  $\Delta S^\circ$  are computed from the slope and intercept of plot (Fig. 8).

Thermodynamic information is summarized in Table 4. The negative values of  $\Delta G^\circ$  in all temperatures indicate that the adsorption is a fairly favorable and spontaneous pro-

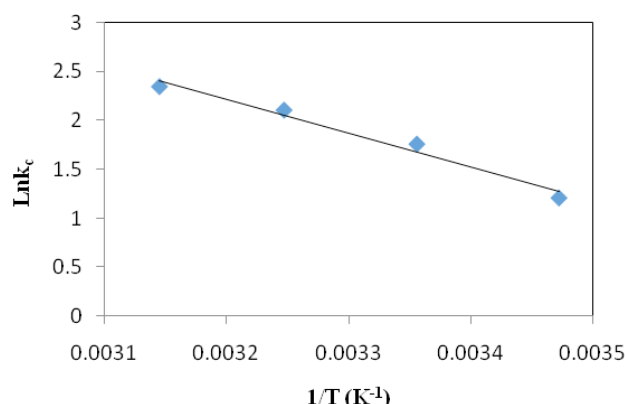


Fig. 8. Plot of  $\ln k_c$  vs.  $1/T$  for estimation of thermodynamic parameters for adsorption of diazinon on CHN-CNT.

Table 4  
Thermodynamic parameters for diazinon adsorption onto CHN-CNT

Adsorbent	Thermodynamic parameters	Temperature				R <sup>2</sup>
		318	308	298	288	
CHN-CNT	$\Delta G^\circ$ (KJ/mol)	-2.88	-4.35	-5.39	-6.21	0.976
	(KJ/mol)	28.9				
	$\Delta S^\circ$ (J/(mol·K))	111				

cess. Also, the decrease in  $\Delta G^\circ$  by the increase in temperatures confirmed that high temperatures would make more spontaneous and faster for the adsorption of diazinon onto CHN-CNT. In other words, high temperatures are favorable [11]. The positive value of  $\Delta H^\circ$  (28.9 kJ/mol) indicates that the adsorption of diazinon onto CHN-CNT is endothermic in nature. The values of standard entropy change  $\Delta S^\circ$  (111 J/mol K) suggest the increasing randomness at the solid/liquid interface [29].

### 3.7. Regeneration of new adsorbent

The regeneration studies will determine the reusability of the CHN-CNT which contributes to the cost-effectiveness of as an adsorbent. Regeneration could be done using several common eluents reported in literatures such as EDTA, hydrochloric acid, nitric acid, sodium chloride solution, and sodium hydroxide [15]. The adsorbent recovery is defined as the percentage ratio of the adsorption capacity of the regenerated adsorbents to that of the initial adsorbent. In this study, the regeneration was done by 0.1 M of NaOH solution, which was known to be efficient in recovery process. In alkaline medium the diazinon adsorption decrease due to protonation of amine groups of chitosan does not occur and the electrostatic repulsion between the surface of diazinon and the surface of CHN-CNT induce. The value of pH was adjusted to 13 and the regeneration time was evaluated to be in the range of 10–30 min. The effect of regeneration cycles of the CHN-CNT on the diazinon adsorption capacity for initial concentration 5 mg/L was examined and the results are shown in Table 5. According to the obtained data, the adsorption capacity before regeneration was about

Table 5  
Regeneration of CHN-CNT for diazinon

Cycle	Adsorption capacity of diazinon (mg/g)		Regeneration efficiency (%)
	Before regeneration	After regeneration	
1	8.25	8.01	97.2
2	8.25	7.9	95.9
3	8.25	7.87	95.4
4	8.25	7.82	94.9

8.25 mg/g. It decreased to 8.01 mg/g after the first cycle of regeneration, and in the fourth cycle of regeneration, it was about 7.82 mg/g. Decrease in adsorption capacity after regeneration may be due to incomplete desorption of the diazinon from the surface of CHN-CNT [29]. The results demonstrated that the CHN-CNT could be effectively regenerated furthermore its regeneration process is simple and cost-effective.

## 4. Conclusions

In this work CHN-CNT was prepared by a protected cross linking method with 2.5% of MWCNT. The results of SEM, FT-IR and TGA tests confirm the bonding of the carbon nanotubes and the chitosan. Diazinon adsorption on CHN-CNT, was examined under different operational parameters. It was found that the adsorption rate of diazinon onto CHN-CNT depended on solution pH value, the amount of CHN-CNT, contact time and solution temperature. The fitting of the equilibrium isotherm data of the CHN-CNT into different isotherm models showed the best fit to the Sips model. The maximum adsorption capacity of the CHN-CNT obtained from the Sips model was 222.86 mg/g. The adsorption kinetics were more appropriately described by the pseudo-second-order model rather than pseudo-first-order model. Also the non-linear forms of pseudo-first-order and pseudo-second-order models were more suitable than the linear forms for fitting the experimental data. Further, the thermodynamic data illustrate that the adsorption process is spontaneous, endothermic. The regeneration of the CHN-CNT could be effectively performed by 0.1 M of NaOH solution, and reused without decreasing its adsorption capacity significantly. Overall, the CHN-CNT exhibited a high regeneration efficiency and excellent removal efficiency in adsorption of diazinon. Therefore, more studies on the removal of other environmental pollutants by CHN-CNT are strongly recommended.

## References

- [1] P. Kabwadza-Corner, N. Matsue, E. Johan, T. Henmi, Mechanism of Diazinon Adsorption on Iron Modified Montmorillonite, *Am. J. Anal. Chem.*, 5 (2014) 70–76.
- [2] WHO, Environmental Health Criteria, 198 - Diazinon. International Programme on Chemical Safety. World Health Organization. Geneva. 140 p., (1998).
- [3] M. Cycon, A. Zmijowska, M. Wojcik, Z. Piotrowska-Seget, Biodegradation and bioremediation potential of diazinon-degrading *Serratia marcescens* to remove other organophosphorus pesticides from soils, *J. Environ. Manage.*, 117 (2013) 7–16.

- [4] R.J. Gilliom, J.E. Barbash, D.W. Kolpin, S.J. Larson, Peer reviewed: testing water quality for pesticide pollution, *Environ. Sci. Technol.*, 33 (1999) 164A–169A.
- [5] M.I. Badawy, M.Y. Ghaly, T.A. Gad-Allah, Advanced oxidation processes for the removal of organophosphorus pesticides from wastewater, *Desalination*, 194 (2006) 166–175.
- [6] N. Ohashi, Y. Tsuchiya, H. Sasano, A. Hamada, Ozonation Products of Organophosphorous Pesticides in Water, *Jpn. J. Tox. Env. Heal.*, 40 (1994) 185–192.
- [7] Kosutic, L. Furaa, L. Sipos, B. Kunst, Removal of arsenic and pesticides from drinking water by nanofiltration membranes, *Sep. Purif. Technol.*, 42 (2005) 137–144.
- [8] Y. Zhang, Y. Hou, F. Chen, Z. Xiao, J. Zhang, X. Hu, The degradation of chlorpyrifos and diazinon in aqueous solution by ultrasonic irradiation: Effect of parameters and degradation pathway, *Chemosphere*, 82 (2011) 1109–1115.
- [9] A.A. Amooey, S. Ghasemi, S.M. Mirsoleimani-azizi, Z. Gholaminezhad, M.J. Chaichi, Removal of Diazinon from aqueous solution by electrocoagulation process using aluminum electrodes, *Korean J. Chem. Eng.*, 31 (2014) 1016–1020.
- [10] A.E. Abo-Amer, Biodegradation of diazinon by *Serratia marcescens* D1101 and its use in bioremediation of contaminated environment, *J. Microbiol. Biotechnol.*, 21 (2011) 71–80.
- [11] G. Moussavi, H. Hosseini, A. Alahabadi, The investigation of diazinon pesticide removal from contaminated water by adsorption onto  $\text{NH}_4\text{Cl}$ -induced activated carbon, *Chem. Eng. J.*, 214 (2013) 172–179.
- [12] K.S. Ryoo, S.Y. Jung, H. Sim, J.-H. Choi, Comparative study on adsorptive characteristics of diazinon in water by various adsorbents, *Bull. Korean Chem. Soc.*, 34 (2013) 27–53.
- [13] M. Armaghan M. Amini, Adsorption of diazinon and fenitrothion on nanocrystalline alumina from non-polar solvent, *Colloid J.*, 74 (2012) 427–433.
- [14] X. Qu, P.J. Alvarez, Q. Li, Applications of nanotechnology in water and wastewater treatment, *Water Res.*, 47 (2013) 3931–3946.
- [15] W.W. Ngah, L. Teong, M. Hanafiah, Adsorption of dyes and heavy metal ions by chitosan composites: A review, *Carbohydr. Polym.*, 83 (2011) 1446–1456.
- [16] S. Moradi Dehaghi, B. Rahmanifar, A.M. Moradi, P.A. Azar, Removal of permethrin pesticide from water by chitosan-zinc oxide nanoparticles composite as an adsorbent, *J. Saud. Chem. Soc.*, 18 (2014) 348–355.
- [17] M.N.R. Kumar, A review of chitin and chitosan applications, *React. Funct. Polym.*, 46 (2000) 1–27.
- [18] A. Aryaei, A.H. Jayatissa, A.C. Jayasuriya, Mechanical and biological properties of chitosan/carbon nanotube nanocomposite films, *J. Biomed. Mater. Res. A.*, 102 (2014) 2704–2712.
- [19] S.-F. Wang, L. Shen, W.-D. Zhang, Y.-J. Tong, Preparation and mechanical properties of chitosan/carbon nanotubes composites, *Biomacromolecules*, 6 (2005) 3067–3072.
- [20] S. Chatterjee, M.W. Lee, S.H. Woo, Adsorption of congo red by chitosan hydrogel beads impregnated with carbon nanotubes, *Bioresour. Technol.*, 101 (2010) 1800–1806.
- [21] S.B. Kim, Y.J. Kim, T.L. Yoon, S.A. Park, I.H. Cho, E.J. Kim, I.A. Kim, J.-W. Shin, The characteristics of a hydroxyapatite-chitosan-PMMA bone cement, *Biomaterials*, 25 (2004) 5715–5723.
- [22] J. Wang, J. De Boer, K. De Groot, Preparation and characterization of electrodeposited calcium phosphate/chitosan coating on  $\text{Ti6Al4V}$  plates, *J. Dent. Res.*, 83 (2004) 296–301.
- [23] L. Carson, C. Kelly-Brown, M. Stewart, A. Oki, G. Regisford, Z. Luo, V.I. Bakhmutov, Synthesis and characterization of chitosan-carbon nanotube composites, *Mater. Lett.*, 63 (2009) 617–620.
- [24] S.R. Popuri, R. Frederick, C.-Y. Chang, S.-S. Fang, C.-C. Wang, L.-C. Lee, Removal of copper (II) ions from aqueous solutions onto chitosan/carbon nanotubes composite sorbent, *Desalin. Water. Treat.*, 52 (2014) 691–701.
- [25] F. Aviles, J. Cauich-Rodriuez, L. Moo-Tah, A. May-Pat, R. Vargas-Coronado, Evaluation of mild acid oxidation treatments for MWCNT functionalization, *Carbon*, 47 (2009) 2970–2975.
- [26] I.D. Rosca, F. Watari, M. Uo, T. Akasaka, Oxidation of multi-walled carbon nanotubes by nitric acid, *Carbon*, 43 (2005) 3124–3131.
- [27] V. Datsyuk, M. Kalyva, K. Papagelis, J. Parthenios, D. Tasis, A. Siokou, I. Kallitsis, C. Galiotis, Chemical oxidation of multi-walled carbon nanotubes, *Carbon*, 46 (2008) 833–840.
- [28] H. Kitamura, M. Sekido, H. Takeuchi, M. Ohno, The method for surface functionalization of single-walled carbon nanotubes with fuming nitric acid, *Carbon*, 49 (2011) 3851–3856.
- [29] S. Skandari, A. Torabian, G.N. Bidhendi, M. Baghdadi, B. Aminzadeh, Preparation of engineered carbon nanotube materials and its application in water treatment for removal of hydrophobic natural organic matter (NOM), *Desal. Water. Treat.*, (2016) 1–12.
- [30] M.-S. Chiou, P.-Y. Ho, H.-Y. Li, Adsorption of anionic dyes in acid solutions using chemically cross-linked chitosan beads, *Dyes. Pigments.*, 60 (2004) 69–84.
- [31] K. Yoshizuka, Z. Lou, K. Inoue, Silver-complexed chitosan microparticles for pesticide removal, *React. Funct. Polym.*, 44 (2000) 47–54.
- [32] W.W. Ngah, C. Endud, R. Mayanar, Removal of copper (II) ions from aqueous solution onto chitosan and cross-linked chitosan beads, *React. Funct. Polym.*, 50 (2002) 181–190.
- [33] H.A. Shawky, A.H.M. El-Aassar, D.E. Abo-Zeid, Chitosan/carbon nanotube composite beads: Preparation, characterization, and cost evaluation for mercury removal from wastewater of some industrial cities in Egypt, *J. Appl. Polym. Sci.*, 125 (2011) E93–E101.
- [34] L. Baldino, S. Concilio, S. Cardea, I. De Marco, E. Reverchon, Complete glutaraldehyde elimination during chitosan hydrogel drying by  $\text{SC-CO}_2$  processing, *J. Supercritical Fluids*, 103 (2015) 70–76.
- [35] B. Li, C.-L. Shan, Q. Zhou, Y. Fang, Y.-L. Wang, F. Xu, L.-R. Han, M. Ibrahim, L.-B. Guo, G.-L. Xie, Synthesis, characterization, and antibacterial activity of cross-linked chitosan-glutaraldehyde, *Marine drugs*, 11 (2013) 1534–1552.
- [36] P.G. Ingole, N.R. Thakare, K. Kim, H.C. Bajaj, K. Singh, H. Lee, Preparation, characterization and performance evaluation of separation of alcohol using crosslinked membrane materials, *New J. Chem.*, 37 (2013) 4018–4024.
- [37] C.d.T. Neto, J. Giacometti, A. Job, F. Ferreira, J. Fonseca, M. Pereira, Thermal analysis of chitosan based networks, *Carbohydr. Polym.*, 62 (2005) 97–103.
- [38] D.Y. Pratt, L.D. Wilson, J.A. Kozinski, Preparation and sorption studies of glutaraldehyde cross-linked chitosan copolymers, *J. Colloid Interface Sci.*, 395 (2013) 205–211.
- [39] L.D. Wilson, C. Xue, Macromolecular sorbent materials for urea capture, *J. Appl. Polym. Sci.*, 128 (2013) 667–675.
- [40] I. Olivas-Armendáriz, E. Santos-Rodríguez, S. Correa-Espinoza, D.-S. Domínguez-Domínguez, I. Márquez-Méndez, M. Mendoza-Duarte, M.-C. Chavarria-Gaytá, S.-A. Martel-Estrada, Evaluation of mechanical and thermophysical properties of chitosan/poly (DL-Lactide-co-Glycolide)/multiwalled Carbon nanotubes for tissue engineering, *Am. J. Mater. Sci.*, 5 (2015) 9–16.
- [41] S.K. Yadav, S.S. Mahapatra, M.K. Yadav, P.K. Dutta, Mechanically robust biocomposite films of chitosan grafted carbon nanotubes via the [2+1] cycloaddition of nitrenes, *RSC Advances*, 3 (2013) 23631–23637.
- [42] A. Jonidi-Jafari, M. Shirzad-Siboni, J.-K. Yang, M. Naimi-Joubani, M. Farrokhi, Photocatalytic degradation of diazinon with illuminated  $\text{ZnO-TiO}_2$  composite, *J. Taiwan Ins. Chem. Eng.*, 50 (2015) 100–107.
- [43] Y.-T. Shieh, C.-M. Wen, R.-H. Lin, T.-L. Wang, C.-H. Yang, Y.-K. Twu, Effects of pH on electrocatalytic activity of carbon nanotubes in poly (acrylic acid) composites used for electrochemical selective detection of uric acid and dopamine in the presence of ascorbic acid, *Int. J. Electrochem. Sci.*, 7 (2012) 8761–8778.
- [44] J. Hu, C. Chen, X. Zhu, X. Wang, Removal of chromium from aqueous solution by using oxidized multiwalled carbon nanotubes, *J. Hazard. Mater.*, 162 (2009) 1542–1550.

- [45] W. Chen, L. Duan, D. Zhu, Adsorption of polar and nonpolar organic chemicals to carbon nanotubes, *Environ. Sci. Technol.*, 41 (2007) 8295–8300.
- [46] Z. Wang, M.D. Shirley, S.T. Meikle, R.L. Whitby, S.V. Mikhalovsky, The surface acidity of acid oxidised multi-walled carbon nanotubes and the influence of in-situ generated fulvic acids on their stability in aqueous dispersions, *Carbon*, 47 (2009) 73–79.
- [47] P.T. Thuy, N.V. Anh, B. Van der Bruggen, Evaluation of two low-cost-high performance adsorbent materials in the waste to product approach for the removal of pesticides from drinking water, *Clean Soil Air Water*, 40 (2012) 246–253.
- [48] G.Z. Memon, M. Bhangar, M. Akhtar, The removal efficiency of chestnut shells for selected pesticides from aqueous solutions, *J. Colloid Interface Sci.*, 315 (2007) 33–40.
- [49] W.W. Ngah S. Fatinathan, Adsorption of Cu (II) ions in aqueous solution using chitosan beads, chitosan-GLA beads and chitosan-alginate beads, *Chem. Eng. J.*, 143 (2008) 62–72.
- [50] L. Poon, S. Younus, L.D. Wilson, Adsorption study of an organo-arsenical with chitosan-based sorbents, *J. Colloid Interface Sci.*, 420 (2014) 136–144.
- [51] L. Wang A. Wang, Adsorption characteristics of Congo Red onto the chitosan/montmorillonite nanocomposite, *J. Hazard. Mater.*, 147 (2007) 979–985.
- [52] A. Kamari, W.W. Ngah, Isotherm, kinetic and thermodynamic studies of lead and copper uptake by H<sub>2</sub>SO<sub>4</sub> modified chitosan, *Colloid. Surface. B.*, 73 (2009) 257–266.
- [53] Y.-H. Li, Z. Di, J. Ding, D. Wu, Z. Luan, Y. Zhu, Adsorption thermodynamic, kinetic and desorption studies of Pb<sup>2+</sup> on carbon nanotubes, *Water Res.*, 39 (2005) 605–609.
- [54] H. Zhu, Y. Fu, R. Jiang, J. Yao, L. Liu, Y. Chen, L. Xiao, G. Zeng, Preparation, characterization and adsorption properties of chitosan modified magnetic graphitized multi-walled carbon nanotubes for highly effective removal of a carcinogenic dye from aqueous solution, *Appl. Surf. Sci.*, 285 (2013) 865–873.
- [55] G. Moussavi, S. Talebi, M. Farrokhi, R.M. Sabouti, The investigation of mechanism, kinetic and isotherm of ammonia and humic acid co-adsorption onto natural zeolite, *Chem. Eng. J.*, 171 (2011) 1159–1169.
- [56] L. Abramian, H. El-Rassy, Adsorption kinetics and thermodynamics of azo-dye Orange II onto highly porous titania aerogel, *Chem. Eng. J.*, 150 (2009) 403–410.
- [57] S. Chowdhury, P. Saha, Adsorption kinetic modeling of safranin onto rice husk biomatrix using pseudo-first- and pseudo-second-order kinetic models: comparison of linear and non-linear methods, *Clean-Soil Air Water*, 39 (2011) 274–282.